

Hydrolytically Degradable PEG-Based Inverse Electron Demand Diels–Alder Click Hydrogels

Nathan H. Dimmitt, Matthew R. Arkenberg, Mariana Moraes de Lima Perini, Jiliang Li, and Chien-Chi Lin*

Cite This: *ACS Biomater. Sci. Eng.* 2022, 8, 4262–4273

Read Online

ACCESS |

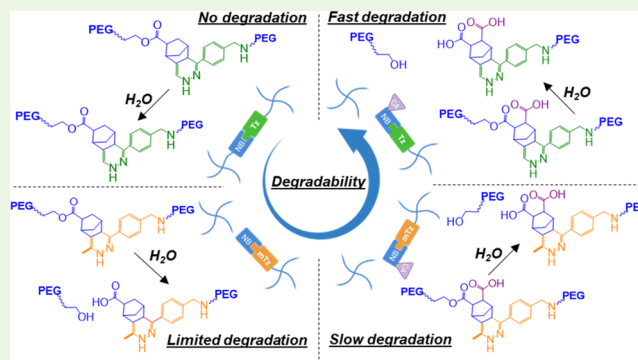
Metrics & More

Article Recommendations

Supporting Information

ABSTRACT: Hydrogels cross-linked by inverse electron demand Diels–Alder (iEDDA) click chemistry are increasingly used in biomedical applications. With a few exceptions in naturally derived and chemically modified macromers, iEDDA click hydrogels exhibit long-term hydrolytic stability, and no synthetic iEDDA click hydrogels can undergo accelerated and tunable hydrolytic degradation. We have previously reported a novel method for synthesizing norbornene (NB)-functionalized multiarm poly(ethylene glycol) (PEG), where carbic anhydride (CA) was used to replace 5-norbornene-2-carboxylic acid. The new PEGNB_{CA}-based thiol-norbornene hydrogels exhibited unexpected fast yet highly tunable hydrolytic degradation. In this contribution, we leveraged the new PEGNB_{CA} macromer for forming iEDDA click hydrogels with [methyl]tetrazine ([m]Tz)-modified macromers, leading to the first group of synthetic iEDDA click hydrogels with highly tunable hydrolytic degradation kinetics. We further exploited Tz and mTz dual conjugation to achieve tunable hydrolytic degradation with an in vitro degradation time ranging from 2 weeks to 3 months. Finally, we demonstrated the excellent in vitro cytocompatibility and in vivo biocompatibility of the new injectable PEGNB_{CA}-based iEDDA click cross-linked hydrogels.

KEYWORDS: hydrogels, iEDDA click reaction, degradation, injectable, cell encapsulation



INTRODUCTION

Hydrogels cross-linked by inverse electron demand Diels–Alder (iEDDA) click reaction are increasingly being developed for applications in controlled release and cell encapsulation.¹ iEDDA click chemistry, a noncatalytic cycloaddition between an electron-rich dienophile (e.g., norbornene, trans-cyclooctene) and an electron-poor diene (e.g., tetrazine, methyltetrazine),^{2,3} proceeds rapidly in ambient conditions and produces a nonlytic adduct with nitrogen gas as the only byproduct. iEDDA click reactions involving norbornene (NB) moiety are particularly useful in creating modularly cross-linked hydrogels owing to the reactivity of NB to free sulfhydryl groups. For example, our group has reported the development of photopolymerized thiol-norbornene hydrogels amenable to a secondary tetrazine-norbornene (Tz-NB) iEDDA click reaction for dynamic hydrogel stiffening.⁴

The irreversibility of the iEDDA click reaction renders the Tz-NB click hydrogels nonhydrolytically degradable, unless degradation motifs are intentionally designed/incorporated in the hydrogel network. The long-term hydrolytic stability of iEDDA hydrogels was demonstrated recently by Goepferich and colleagues with an 8-arm poly(ethylene glycol)-tetrazine (PEGTz) and PEG-norbornene (PEGNB) synthesized via Steglich esterification.⁵ As the hydrolysis rate of ester bonds

formed by Steglich esterification is known to be extraordinarily slow,⁶ no noticeable hydrogel degradation was observed before 100–400 days (depending on the formulations) and the time for complete gel degradation in vitro ranged from ~150 to 500 days. The long-term stability of Tz-NB click hydrogels could also be attributed to the noncovalent secondary supramolecular interactions between the Tz-NB adducts. For example, Alge and colleagues demonstrated slow gelation between the 4-arm PEGNB and linear monofunctional methoxy-PEG-Tz (gel point ~7 min at 21 °C). Unlike conventional thiol-norbornene cross-linked PEG-based hydrogels, PEG-based iEDDA cross-linked hydrogels were found to resist hydrolysis induced by a strong base (0.1 N NaOH).^{7,8}

If desirable, iEDDA click hydrogels may be rendered enzymatically degradable via incorporating protease-labile linkers or peptides. The Anseth group first described the cross-linking of biomimetic peptide-cross-linked iEDDA click

Received: June 24, 2022

Accepted: August 15, 2022

Published: September 8, 2022



hydrogels using multiarm PEGTz and bis-norbornene-modified peptide cross-linkers.⁹ The Tz-NB hydrogels reached G'/G'' crossover within minutes and demonstrated a high cytocompatibility for in situ encapsulation of human mesenchymal stem cells (hMSCs). The Mooney group later modified alginate with Tz or NB groups for their cross-linking into iEDDA click hydrogels.¹⁰ The cell adhesive peptide (e.g., CGGGGRGDSP) was photoconjugated to the norbornene group to permit cell adhesion on the otherwise non-cell-adhesive alginate hydrogels. As alginate was not degradable by mammalian proteases, oligopeptide (e.g., GCRD-VPMSMRGG-DRCG)^{11,12} or Tz/NB-modified gelatin (Gel-Tz and Gel-NB) was cross-linked to permit cell-mediated matrix degradation.^{13,14} In particular, gelatin-based “ClickGels” achieved gelation in minutes, demonstrated high cell attachment and viability for hMSCs and 3T3 fibroblasts, were enzymatically degradable, and were capable of being injected in vivo.¹⁴ Similarly, the Shoichet group conjugated methylphenyltetrazine (mTz) onto hyaluronic acid (HA-mTz) via amide coupling, permitting iEDDA click cross-linking of HA-based hydrogels that were sensitive to hyaluronidase-mediated degradation.¹⁵

In addition to using protease-labile linkers, iEDDA click cross-linked hydrogels can be designed to contain linkers susceptible to oxidation, such as disulfide exchange. For example, the Shoichet group synthesized dithiopropionic acid dihydrazide (DTP) and methylphenyltetrazine containing methylcellulose (i.e., MC-DTP-mTz).¹⁶ Addition of glutathione (GSH) to the MC-based iEDDA hydrogels led to disulfide exchange-induced hydrogel degradation. Similarly, Vu and colleagues installed the disulfide bond in a bifunctional tetrazine PEG cross-linker for GSH-triggered release of doxorubicin (DOX), an anticancer drug, from alginate-based iEDDA click hydrogels.¹⁷ These exogenously triggered degradation strategies, however, cannot be easily controlled in an in vivo setting, where hydrogels with pre-engineered degradation kinetics may be beneficial to tissue regeneration. In this regard, iEDDA click cross-linked hydrogels with engineered ester hydrolysis kinetics will significantly benefit the use of iEDDA click hydrogels as injectable and degradable scaffolds for in vivo tissue regeneration. For example, Lueckgen et al. rendered the saccharide units of alginate chains susceptible to hydrolysis via sequential oxidation and reduction, followed by conjugating NB and Tz to the modified alginates.¹⁸ While the resulting alginate-based Tz-NB hydrogels were found to undergo hydrolytic degradation, the degradation was slow and not precisely engineered.

We have previously reported a new class of NB-modified PEG-based macromers (i.e., PEGNB_{CA}) for forming thiol-norbornene photoclick hydrogels with fast and tunable hydrolytic degradation kinetics.¹⁹ PEGNB_{CA} was synthesized by reacting the hydroxyl-terminated multiarm PEG with carbic anhydride (CA). Hydrogels cross-linked by PEGNB_{CA} possessed the same characteristics of rapid cross-linking and spatiotemporal tunability afforded by the thiol-norbornene photopolymerization, while providing accelerated ester hydrolysis rates when compared with conventional PEGNB hydrogels. Critically, the new PEGNB_{CA} hydrogels supported in situ encapsulation and growth of cancer cells and stem cells, including human induced pluripotent stem cells (hiPSCs). In this report, we leveraged PEGNB_{CA} to fabricate and engineer the first PEG-based iEDDA click hydrogels susceptible to accelerated and highly tunable hydrolytic degradation.

MATERIALS AND METHODS

Materials. The hydroxyl-terminated 8-arm PEG (20 kDa) and 4-arm PEG-amino succinic acid (PEG-ASA) (10 kDa) were purchased from JenKem Technology and Laysan Bio Inc., respectively. Carbic anhydride, pyridine, dichloromethane (DCM), and 1-(3-dimethylaminopropyl)-3-ethylcarbodiimide hydrochloride (EDC) were all purchased from Thermo Scientific. 5-Norbornene-2-carboxylic acid, tetrahydrofuran (THF), 4-dimethylaminopyridine (DMAP), and *N,N'*-dicyclohexylcarbodiimide (DCC) were obtained from Sigma-Aldrich. Tetrazine-amine and methyltetrazine-amine were purchased from Click Chemistry Tools. *N*-hydroxysuccinimide (NHS) and *N,N*-diisopropylethylamine (DIEA) were obtained from Tokyo Chemical Industry (TCI). *N,N*-dimethylformamide (DMF), 1-[bis(dimethylamino)methylene]-1*H*-1,2,3-triazolo[4,5-*b*]pyridinium 3-oxide hexafluorophosphate (HATU), and cold soluble gelatin were purchased from Alfa Aesar, AnaSpec, and Modernist Pantry, respectively. Calcein-AM and ethidium homodimer stains were obtained from Biotium. F-actin stain was purchased from Cytoskeleton, Inc.

Macromer Synthesis and Purification. *Synthesis of PEGNB and PEGNB_{CA}.* The 8-arm PEGNB was synthesized according to an established protocol.^{20,21} Briefly, 10 parts of norbornene acid were reacted with 5 parts of DCC in DCM to form norbornene anhydride with dicyclohexylurea as a byproduct. Dicyclohexylurea was removed through vacuum filtration with a filter paper (size 52). Norbornene anhydride was then added dropwise into a flask containing hydroxyl-terminated 8-arm PEG (20 kDa), pyridine (10-fold to $-OH$), and DMAP (1-fold to $-OH$). All reactions occurred under nitrogen gas and the product was precipitated with diethyl ether and filtered using a fritted glass funnel. The PEGNB product was redissolved in double-distilled water (DDH₂O). The 8-arm PEGNB-carbic anhydride (PEGNB_{CA}) was synthesized using our published protocol.^{19,22} Briefly, the hydroxyl-terminated 8-arm PEG (20 kDa) was reacted with 5-fold carbic anhydride and 0.5-fold DMAP in THF at 60 °C for 12 h. After 12 h, a second portion of 5-fold carbic anhydride and 0.5-fold DMAP was added and proceed to react for another 24 h. The PEGNB_{CA} product was precipitated with diethyl ether and redissolved in DDH₂O.

Synthesis of PEGTz, PEG-mTz, and PEG-mTz/Tz. Tetrazine-amine (Tz-amine) and/or methyltetrazine-amine (mTz-amine) were conjugated onto the 4-arm PEG-ASA (10 kDa) following a previously reported protocol.⁴ Briefly, PEG-ASA and 5-fold HATU was dissolved in DMF and allowed to react in order to form an active ester. Subsequently, either 1.2-fold Tz-amine or mTz-amine and 5-fold DIEA were added and allowed to react for 16 h at room temperature. Similar to PEGTz and PEG-mTz syntheses, dual-functional PEG-mTz/Tz ratios were obtained by the one-pot reaction of various molar ratios of methyltetrazine-amine and tetrazine-amine on the 4-arm PEG-ASA. The feed molar ratios between mTz-amine and Tz-amine were controlled at 1:3, 1:1, and 3:1.

Gel-mTz/Tz synthesis: Cold soluble gelatin solution (0.5 g in 10 mL DDH₂O), EDC (0.15 mmol), and NHS (0.15 mmol) were first added and allowed to react for 30 min. Equal moles of Tz-amine and mTz-amine (0.075 mmol) were then added to the reaction flask and reacted overnight. The crude product was dialyzed with SpectraPor regenerated cellulose dialysis membrane with a molecular weight cutoff (MWCO) of 3.5 kDa for 3 days, lyophilized, and stored at -20 °C until use.

Macromer Characterization. The substitution of norbornene onto the 8-arm PEG was done using ¹H NMR (deuterium oxide, 500 MHz, Bruker Advance 500) by obtaining the integral peaks of the protons on the PEG backbone to the alkene protons on the norbornene group. Substitution of tetrazine and/or methyltetrazine onto PEG-ASA and cold soluble gelatin was done using ultraviolet-visible (UV-vis) spectroscopy against a standard curve (1–0.015 mg/mL) of the respected ratio of free Tz-amine and/or mTz-amine. At these low concentrations, both Tz-amine and mTz-amine were completely soluble in water. The actual ratio of Tz and mTz conjugated onto PEG-ASA was determined by comparing the integral

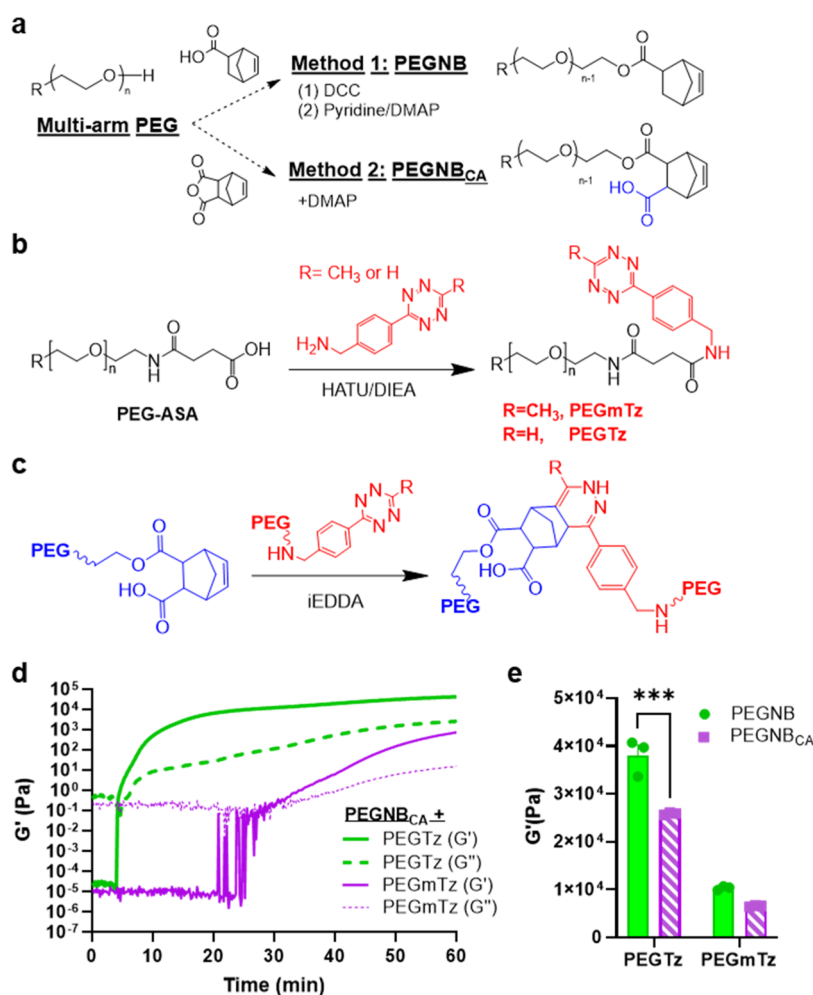


Figure 1. Cross-linking of PEG-based iEDDA click hydrogels using PEGNB or PEGNB_{CA}. (a) Synthesis of norbornene-functionalized multiarm PEG macromers: method 1: PEGNB and method 2: PEGNB_{CA}. (b) Synthesis of (methyl)tetrazine-functionalized multiarm PEG (R = CH₃, PEGmTz; R = H, PEGTz). (c) iEDDA click reaction between PEGNB_{CA} and PEGTz/PEGmTz. (d) In situ rheometry of iEDDA click hydrogel cross-linking using PEGNB_{CA} with PEGTz or PEGmTz. (e) Shear moduli of 2.5 wt % PEGNB_{CA} or PEGNB cross-linked with either PEGTz or PEGmTz (R = 1). ****p* < 0.001.

peaks of the protons on the benzyl ring to the integral peaks on the methyl group of mTz.

Hydrogel Cross-linking and Degradation. PEGNB or PEGNB_{CA} was cross-linked with PEGTz, PEGmTz, or PEG-mTz/Tz with stoichiometric ratios of [Tz] to [Nb] (i.e., R) at 0.5, 1.0, or 2.0 at a fixed PEGNB macromer concentration of 2.5 wt %, as well as different PEGNB macromer concentrations (i.e., 1.75, 2.5, and 4 wt %) at a fixed stoichiometric ratio of 1. To prepare hydrogels, 45 μ L of polymer precursor solution was injected between two glass slides separated by 1 mm Teflon spacers. The slides containing the hydrogel precursor solution were then placed into a sealed container and allowed to react for 16 h at room temperature. After 16 h, the hydrogels were swelled in pH 7.4 phosphate-buffered saline (PBS). Using an Anton-Paar MCR102 rheometer fitted with an 8 mm diameter parallel geometry plate, elastic (G') and viscous (G'') moduli of the fabricated hydrogels were evaluated through strain sweep tests operating at 0.1–5% strain and 1 Hz oscillation frequency. The gelation kinetics was determined using in situ rheometry performed with a 25 mm diameter parallel geometry plate. The hydrogel precursor solution was mixed briefly, and then 200 μ L of the solution was dispensed on the rheology stage. The plate was lowered to a gap size of 0.2 mm and time sweep was conducted at 1% strain and 1 Hz frequency over 1 h. In situ rheology was performed either at 25 or at 37 $^{\circ}$ C.

Cell Encapsulation and Analysis. hMSC Culture. Adherent human mesenchymal stem cells (hMSCs) were isolated from donor bone marrow (acquired from Lonza) and cultured in low-glucose (1 g/L) Dulbecco's modified Eagle's medium (DMEM) supplemented with 10% fetal bovine serum (FBS), 1% antibiotic-antimycotics, and 1 ng/mL basic fibroblast growth factor (bFGF). The media was changed every 3–4 days. Once cell confluency reached \sim 80%, cells were passaged using trypsin. hMSCs were used at passage numbers 4–6.

Cell Encapsulation. All polymers were sterilized by sterile filtering through a membrane with 0.22 μ m pore size. Detached and dispersed hMSCs were encapsulated in 2.5 wt % PEGNB or PEGNB_{CA} hydrogels cross-linked with PEG-25mTz/75Tz at R = 0.5. To improve the biocompatibility, 3 wt % Gel-50mTz/50Tz was reacted 1 h before at 37 $^{\circ}$ C before gelation occurred. After 7 min of reacting at 37 $^{\circ}$ C for PEGNB_{CA} hydrogels and 2 min for PEGNB hydrogels, 25 μ L of the hydrogel precursor solution containing hMSCs was placed in open-tip 1 mL syringes. The cell-laden hydrogels were then allowed to react for another 20 min before being placed in cell culture media. As before, media changes occurred every 3–4 days.

Live/Dead and F-actin/DAPI Staining. On day 1 and day 14, cell-laden hydrogels were washed with Dulbecco's PBS (DPBS) for 5 min. Next, the cell-laden hydrogels were incubated with 0.3 μ L/mL of Calcein-AM and 0.26 μ L/mL of ethidium homodimer for 1 h at room temperature protected from light. After 1 h, the cell-laden hydrogels

were washed three times for 5 min using DPBS. On day 14, the cell-laden hydrogels were washed twice for 5 min with DPBS and fixed with 4% paraformaldehyde for 45 min. Fixed cells within the hydrogel were then stained with 140 nM of F-actin (Acti-stain 555 Fluorescent Phalloidin, Cytoskeleton, Inc.) in the presence of 1% (v/v) bovine serum albumin (BSA) and 0.3% (v/v) Triton X100 at 4 °C overnight. F-actin-stained cells in the hydrogel were washed three times for 30 min with 1% (v/v) BSA and 0.3% (v/v) Triton X100, and then counterstained with DAPI for 1 h at room temperature. The stained cells in the hydrogel were washed with DPBS, and then imaged using confocal microscopy (Olympus Fluoview, FV1000). For analysis, a total of three hydrogels were imaged per condition with at least three random images per gel.

Image Analysis. ImageJ was used to quantify the morphology of the F-actin/DAPI-stained hMSCs in PEGNB and PEGNB_{CA} hydrogels. Briefly, images were processed using fill holes and watershed features. Subsequently, the analyze particle feature was applied with the appropriate size threshold set and shape descriptor for each image. Circularity was calculated using the following equation

$$\text{circularity} = \frac{4\pi \text{Area}}{\text{perimeter}^2} \quad (1)$$

Aspect ratio was also calculated through ImageJ using the equation

$$\text{aspect ratio} = \frac{\text{width}^2}{\text{area}} \quad (2)$$

In Vivo Injection and Histological Evaluation. All animal studies were approved by the Indiana University-Purdue University Indianapolis School of Science Institutional Animal Care and Use Committee (Approval number: SC303R). A total of six C57BL/6 mice were used. All polymers were sterilized by sterile filtering through a membrane with 0.22 μm pore size before injection. PEGNB_{CA} and PEGNB were prereacted with Gel-mTz/Tz for 1 h at 37 °C. Next, the PEG-mTz/Tz macromer was added to PEGNB_{CA}/Gel-mTz/Tz solution and allowed to react for 8 min at 37 °C before injection. As PEGNB reacted faster, the PEG-mTz/Tz macromer was added to the PEGNB solution and allowed to react for 2 min at room temperature before injection. Under sterile conditions, 50 μL of 2.5 wt % PEGNB or PEGNB_{CA} cross-linked with PEG-25mTz/75Tz with *R* = 0.8 and 3 wt % Gel-50mTz/50Tz was injected into the region of the quadriceps muscle of the left hindlimb of each mouse. The body weights of the mice were measured weekly. After two weeks, mice were sacrificed and the quadriceps muscle from the left hindlimb was collected. The collected muscle tissue was fixed in formalin for one day and subsequently stored in 70% ethanol. Tissue specimens were embedded in paraffin, sectioned, and stained with hematoxylin and eosin (HE), CD45 (Cell Signaling Technology, Rabbit mab), and CD68 (Cell Signaling, Rabbit mab). Images were processed using ImageJ to calculate the area positive for either CD45 or CD68.

Statistics. The data is presented as mean ± standard error of the mean (SEM). When there are more than two conditions, one-way ANOVA or two-way ANOVA with Tukey multiple comparison test was used to determine the statistical significance between groups when *p* < 0.05. When there are only two conditions, unpaired *t*-test was used to determine the statistical significance with *p* < 0.05. Using GraphPad Prism 9, normalized elastic moduli data over time was fitted to a one-phase decay. From here, *k*_{hydrolysis} constants and *R*² values were obtained.

RESULTS

Cross-linking of PEG-Based iEDDA Click Hydrogels. Norbornene-functionalized PEG can be synthesized by reacting hydroxyl-terminated PEG with either 5-norbornene-2-carboxylic acid (NB-acid) or carbic anhydride (CA) (Figure 1a). We have previously demonstrated that thiol-norbornene photoclick hydrogels cross-linked by PEGNB_{CA} degraded unexpectedly fast.¹⁹ In this work, we sought to exploit the accelerated degradation of hydrogels cross-linked by PEGNB_{CA}

and establish the first hydrolytically degradable PEG-based iEDDA click hydrogels. We found that the CA synthesis route produced a high degree of NB substitution efficiency (~91%, ca. 3.6 mM per wt % macromer), a value similar to that of PEGNB synthesized through conventional Steglich esterification between PEG and NB-acid (~95%, ca. 3.8 mM per wt %) (Figure S1). To afford iEDDA click hydrogel cross-linking, we conjugated mTz-amine or Tz-amine to the 4-arm PEG-ASA using standard carbodiimide chemistry with HATU as the acid activator (Figure 1b). NMR and UV-vis spectrophotometry (at 523 nm) analyses showed that (m)Tz-modified PEGs were synthesized with a high degree of substitution efficiency (~85% for PEGTz to 95% for PEG-mTz, data not shown).

The cross-linking of the iEDDA click hydrogel occurred upon simple mixing of PEGNB_{CA} and PEG(m)Tz (Figure 1c). In particular, when 2.5 wt % of PEGNB_{CA} was mixed with PEG(m)Tz at a stoichiometric ratio (*R*) of 1, the *G'*/*G''* crossover time was ~4 min for PEGTz, whereas that for PEG-mTz hydrogels was slower, at ~30 min (Figure 1d). The initial shear moduli of PEGNB_{CA}/PEGTz hydrogels (*G'*) were ~26 kPa, a value lower than that obtained from hydrogels cross-linked by conventional PEGNB (*G'* ~ 38 kPa, Figure 1e). Compared with PEGNB, the lower cross-linking efficiency of hydrogels cross-linked by PEGNB_{CA} was similar to that observed in hydrogels prepared from thiol-norbornene photocross-linking.¹⁹ PEGNB hydrogels cross-linked with PEG-mTz showed a slightly higher but not statistically significant difference in *G'* (~10 kPa) than those cross-linked by PEGNB_{CA} (*G'* ~ 6.5 kPa) (Figure 1e). After one day of swelling, the average *G'* of PEGNB_{CA} hydrogels cross-linked with PEG-mTz increased to over 8 kPa, whereas, that of PEGNB hydrogels was essentially the same (data not shown).

Hydrolytic Degradation of PEG-Based iEDDA Click Hydrogels. The degradation of synthetic PEG-based NB-Tz click hydrogels was possible due to the presence of the ester bond on PEGNB or PEGNB_{CA} (Figure 2a). However, iEDDA click hydrogels cross-linked by PEGNB and PEGTz showed little degradation over the course of 80 days (PEGNB + PEGTz) (Figure 2b). PEGNB + PEG-mTz iEDDA click hydrogels degraded noticeably faster than those with PEGTz, with a pseudo-first-order hydrolysis rate constant (*k*_{hyd}) of ~0.0114 day⁻¹ (Table 1). More strikingly, iEDDA click hydrogels cross-linked by PEGNB_{CA} with either PEGTz or PEG-mTz exhibited a fast hydrolysis rate. Surprisingly, however, PEGNB_{CA} + PEG-mTz iEDDA click hydrogels degraded much slower than PEGNB_{CA} + PEGTz hydrogels, with complete degradation occurring on day 80 and day 18 and *k*_{hyd} values of 0.0481 and 0.1021 day⁻¹, respectively. Gel fractions were obtained to show a similar degree of cross-linking efficiency between PEGTz and PEG-mTz with PEGNB_{CA} (Figure S2a). The hydrogel mass was tracked over time to determine the swelling ratio and the mode of hydrogel degradation (e.g., surface erosion or bulk degradation; Figure S2b). Due to increased swelling ratio within the 28-day period for PEGNB_{CA} + PEGTz hydrogels, we reasoned that the hydrogels degraded following a bulk degradation mechanism.

Engineering the Cross-linking and Degradation of PEG-Based iEDDA Click Hydrogels. Encouraged by the discovery that using PEGTz or PEG-mTz led to strikingly different hydrolytic degradation kinetics in PEGNB/PEGNB_{CA}-based iEDDA click hydrogels, we synthesized mTz/Tz dually modified PEG macromers in an optimized

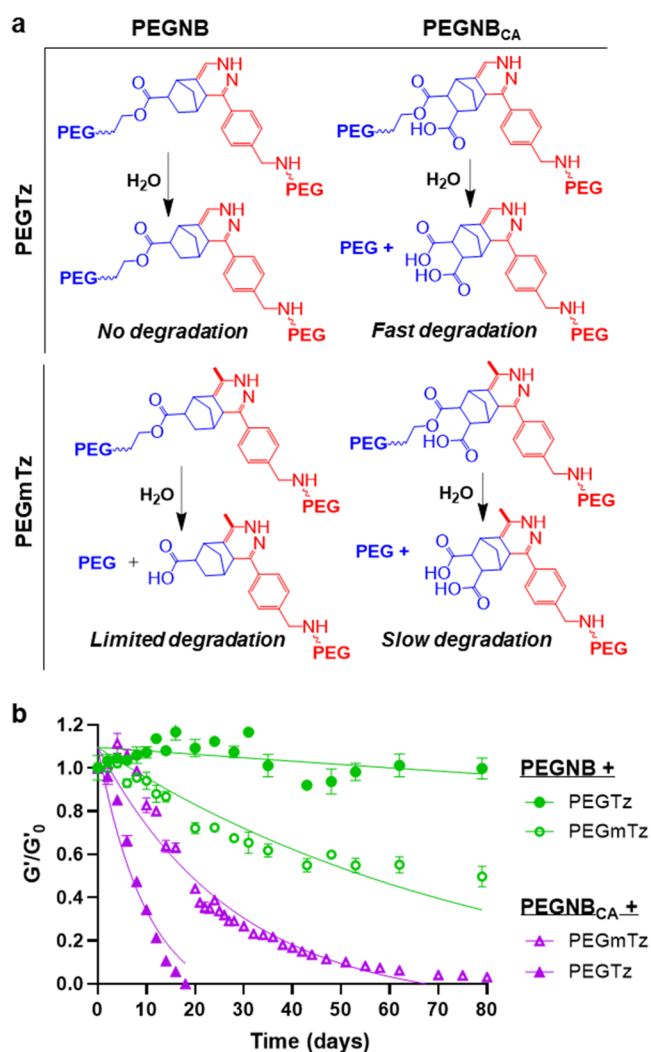


Figure 2. Hydrolytic degradation of PEG-based iEDDA click hydrogels. (a) Hydrolysis scheme. (b) Characterization of hydrogel degradation via shear moduli change (i.e., G'/G_0) as a function of time. The curves' fitting represents the best fit of the pseudo-first-order hydrolytic degradation kinetics.

Table 1. Pseudo-First-Order Hydrolytic Degradation Kinetics of iEDDA Click Hydrogels Cross-linked by PEGNB or PEGNB_{CA}^a

NB macromer	m(Tz) macromer	k_{hyd} (day ⁻¹)	ester hydrolysis	half-life (day)	R^2
PEGNB	PEGTz	N/A	+	N/A	-0.35
	PEG-mTz	0.0114	++	60.69	0.88
PEGNB _{CA}	PEG-mTz	0.0481	+++	14.41	0.97
	PEGTz	0.1021	++++	6.788	0.86

^aAll NB macromers were fixed at 2.5 wt % with an NB/(m)Tz stoichiometric ratio of 1.

engineer the degradation kinetics of iEDDA click hydrogels. mTz/Tz dually modified PEGs were synthesized by controlling the feed ratios of methyltetrazine-amine (mTz-amine) to tetrazine-amine (Tz-amine), yielding three sets of macromers with 75–25, 50–50, and 25–75% (% represents the molar feed ratio of mTz to Tz) (Figure 3a). The actual functional group ratios were determined by NMR spectra using the integral peaks from the protons on the methyl group to the

protons on the benzene ring (Figure S3, 85–15, 69–31, and 35–65%, respectively). PEG-75mTz/25Tz, PEG-50mTz/50Tz, and PEG-25mTz/75Tz will now be labeled as PEG-85mTz/15Tz, PEG-69mTz/31Tz, and PEG-35mTz/65Tz, respectively. The substitution efficiencies, as determined spectrophotometrically (at 523 nm), were ~93% (ca. 3.7 mM per wt %) for PEG-85mTz/15Tz and PEG-69mTz/31Tz, and ~85% (ca. 3.4 mM per wt %) for PEG-35mTz/65Tz.

In situ rheology was performed to determine the gelation point of PEGNB_{CA} compared to PEGNB cross-linked with the PEG-mTz/Tz cross-linker. The iEDDA click cross-linked PEGNB_{CA} hydrogels demonstrated slower gelation times with G'/G'' crossover at ~11 min compared to PEGNB hydrogels with crossover point at ~4 min (2.5 wt % PEGNB with PEG-69mTz/31Tz at $R = 1$, 37 °C; Figure 3b). Different gelation times were observed using the three mTz/Tz cross-linkers (Figure 3c). The G'/G'' crossover time for 2.5 wt % PEGNB_{CA} cross-linked with PEG-35mTz/65Tz, PEG-69mTz/31Tz, and PEG-85mTz/15Tz (at $R = 1$ and 37 °C) was ~7, ~11, and ~18 min, respectively. Further, the iEDDA click cross-linked PEGNB_{CA} demonstrated temperature-sensitive gelation behavior (Figure 3d). For 2.5 wt % PEGNB_{CA} hydrogels cross-linked with PEG-69mTz/31Tz ($R = 1$), the G'/G'' crossover time was ~24 min at 25 °C compared to ~11 min at 37 °C.

As with other click-based hydrogels, the initial G' could be readily tuned by varying the polymer weight percent and the ratio between tetrazine and norbornene (Figure 3e,f). At a constant R , PEGNB_{CA} cross-linked with PEG-35mTz/65Tz had significantly higher elastic moduli compared to equivalent hydrogels cross-linked with PEG-69mTz/31Tz and PEG-85mTz/15Tz. The same trend was observed at different R ratios besides at $R = 2$, where the initial G' for all three macromers showed no statistically significant difference. Further, no statistical difference was observed in the gel fraction and initial swelling ratio of PEGNB_{CA} cross-linked with the various PEG-mTz/Tz hydrogels (Figure S4a,b). However, hydrogels cross-linked by PEGNB_{CA} and PEG-85mTz/15Tz supported a slightly higher mesh size compared to PEGNB_{CA} cross-linked with PEG-69mTz/31Tz or PEG-35mTz/65Tz (Figure S4c).

To assess the hydrolytic degradation of PEGNB_{CA}-based iEDDA click hydrogels, the fabricated hydrogels were swelled in PBS pH 7.4 at 37 °C and elastic moduli were tracked over time. In general, the degradation kinetics were governed by the supramolecular interactions between Tz-NB adducts (Figure 4a) and the hydrolysis kinetics of ester bonds on PEGNB_{CA} (Figure 4b). At a lower PEGNB_{CA} concentration (e.g., 1.75 wt %, $R = 1$), the hydrogels exhibited significant stiffening during the first week (Figure S5a), followed by accelerated degradation over 30–60 days. In addition, increasing the mTz content in PEG-mTz/Tz led to slower degradation (Figure 4c–h). At higher PEGNB_{CA} concentration (e.g., 2.5 and 4 wt % at $R = 1$), no stiffening was observed (Figure S5b,c). At the high R ratio ($R = 2$), the initial stiffening was not significant (Figure S5d), but at the low R ratio ($R = 0.5$), significant stiffening was observed (Figure S5e). Further, the relative content of mTz/Tz determined the degradation rates (Figure 4c–h). For instance, for 4 wt % PEGNB_{CA} cross-linked with PEG-35mTz/65Tz, PEG-69mTz/31Tz, and PEG-85mTz/15Tz, the hydrogels completely degraded within 28, 55, and 80 days with k_{hyd} values of 0.1186, 0.0778, and 0.0486 day⁻¹, respectively (Table S1). The hydrolytic degradation of

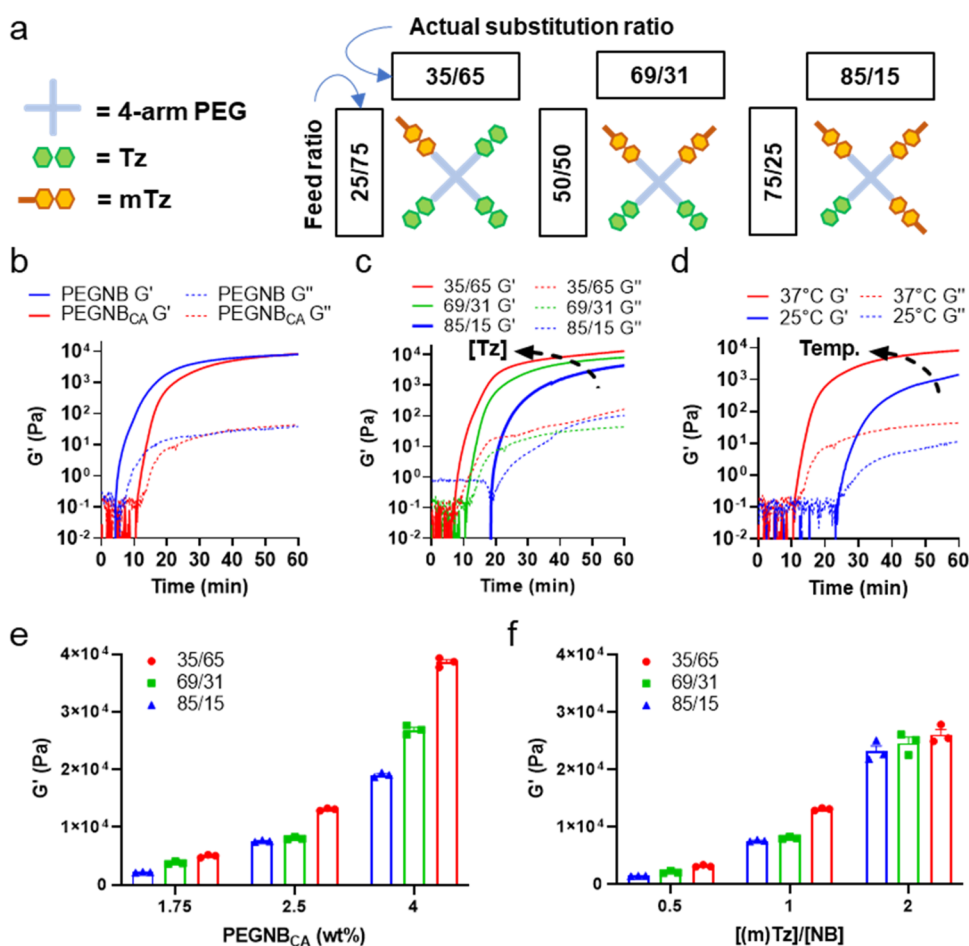


Figure 3. Cross-linking of PEGNB/PEGNB_{CA} iEDDA click hydrogels with dual-functional (m)Tz macromers. (a) Schematics of mTz/Tz dual-functionalized PEG macromers. (b) In situ rheometry of PEGNB or PEGNB_{CA} (2.5 wt %) gel cross-linking using PEG-50mTz/50Tz at 37 °C ($R = 1$). (c) In situ rheometry of PEGNB_{CA} (2.5 wt %) gel cross-linking using PEG-mTz/Tz at different mTz/Tz ratios at 37 °C. (d) In situ rheometry of PEGNB_{CA} (2.5 wt %) gel cross-linking using PEG-mTz/Tz cross-linkers ($R = 1$). (e) Effect of PEGNB_{CA} wt% on the shear modulus of PEGNB_{CA} hydrogels with different PEG-mTz/Tz macromers. Hydrogel shear moduli were measured after 1 h of swelling.

PEGNB_{CA}-based hydrogels was inversely proportional to the R ratio. For example, hydrogels cross-linked with PEG-85mTz/15Tz at $R = 0.5, 1,$ and 2 (Figure 4e) proceeded with k_{hyd} values of $0.1930, 0.0532,$ and 0.0281 day^{-1} , respectively (Table S1). The swelling ratio was tracked over time as another method for observing the rate of hydrolysis. Over a 50-day period, PEGNB_{CA} hydrogels cross-linked with PEG-69mTz/31Tz or PEG-85mTz/15Tz had a swelling ratio twice as large as their initial values, while PEGNB_{CA} + PEG-35mTz/65Tz hydrogels achieved the maximum swelling ratio on day 38, followed by complete degradation the next day (Figure S6).

Three-Dimensional (3D) Encapsulation of hMSCs in iEDDA Click Cross-linked PEG Hydrogels. To test the cytocompatibility of the iEDDA click cross-linked PEGNB_{CA} hydrogels, hMSCs were encapsulated in 2.5 wt % PEGNB_{CA} or PEGNB hydrogels cross-linked by PEG-35mTz/65Tz with $R = 0.5$. Additionally, gelatin functionalized with 50mTz/50Tz (3 wt %) was added to provide cell adhesion and protease-labile sequences. Live/dead staining and confocal imaging demonstrated the excellent cytocompatibility of both PEGNB_{CA} and PEGNB-based hydrogels, with both gels supporting higher than 95% of viable cells one day post encapsulation (Figure 5a). After 14 days of culture, hMSCs displayed an extensive spreading morphology only within the highly degradable PEGNB_{CA} hydrogels, whereas the cells remained largely

rounded in the relatively stable PEGNB hydrogels. The difference in morphology between the two gel formulations was evaluated using anti-F-actin and DAPI staining on day 14 (Figure 5b), which reaffirmed the extensive spreading morphology of hMSCs within the iEDDA click cross-linked PEGNB_{CA} hydrogels. Image analysis demonstrated the statistical difference in aspect ratio and circularity between the two conditions (Figure 5c,d). The mass of iEDDA click cross-linked PEGNB and PEGNB_{CA} hydrogels with gelatin was measured in the presence of collagenase to demonstrate that both hydrogels were equally susceptible to proteolytic degradation (Figure S7a). Further, strain sweep tests were performed on day 1, day 7, and day 14 (Figure S7b). Initially, iEDDA click cross-linked PEGNB_{CA} hydrogels had an average shear modulus greater than 4 kPa. After 14 days, the average elastic modulus was ~ 0.5 kPa. Alternatively, iEDDA click cross-linked PEGNB hydrogels had an average shear modulus close to 3 kPa. On day 7 and day 14, the average shear moduli decreased compared to day 1 due to the quick degradation of gelatin in nonsterile conditions causing the shear moduli to decrease to ~ 2 kPa. The inclusion of the gelatin component was necessary as it provided cell adhesive ligands and protease degradation sites. In the presence of encapsulated cells, one could expect that the degradation of gelatin eventually would lead to reduction of hydrogel cross-linking density.^{13,14} Since

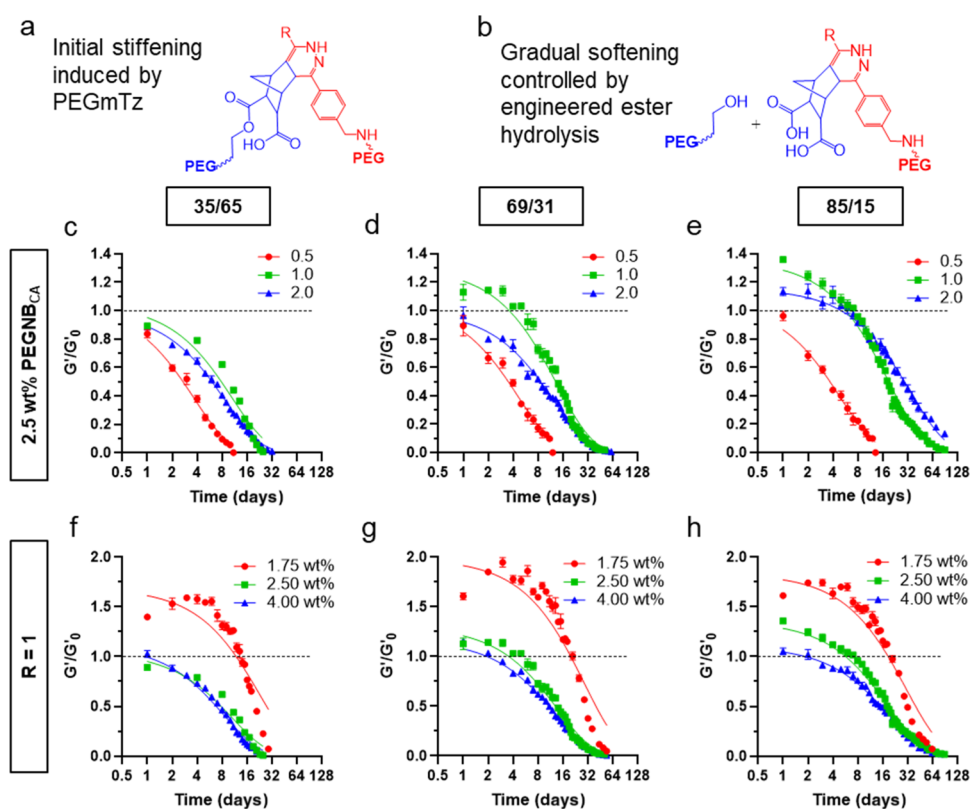


Figure 4. Hydrolytic degradation of PEGNB_{CA}-based iEDDA click hydrogels. (a) Schematic of delayed supramolecular interactions of PEG-mTz with PEGNB_{CA} causing hydrogel stiffening over time. (b) Schematic of ester hydrolysis of iEDDA PEGNB_{CA} hydrogels causing hydrogel softening over time. PEGNB_{CA} was cross-linked with PEG-mTz/Tz ratios of 2.5 wt % with R at 0.5, 1.0, and 2.0 (c: PEG35mTz/65Tz, d: PEG-69mTz/31Tz, and e: PEG85mTz/15Tz). PEGNB_{CA}-PEG-mTz/Tz ratio of hydrogels at different weight percents (1.75, 2.5, and 4 wt %) at R = 1 (f: PEG85mTz/15Tz, g: PEG69mTz/31Tz, and h: PEG-35mTz/65Tz). The values of G'_0 were obtained on day 0 after 1 h of swelling.

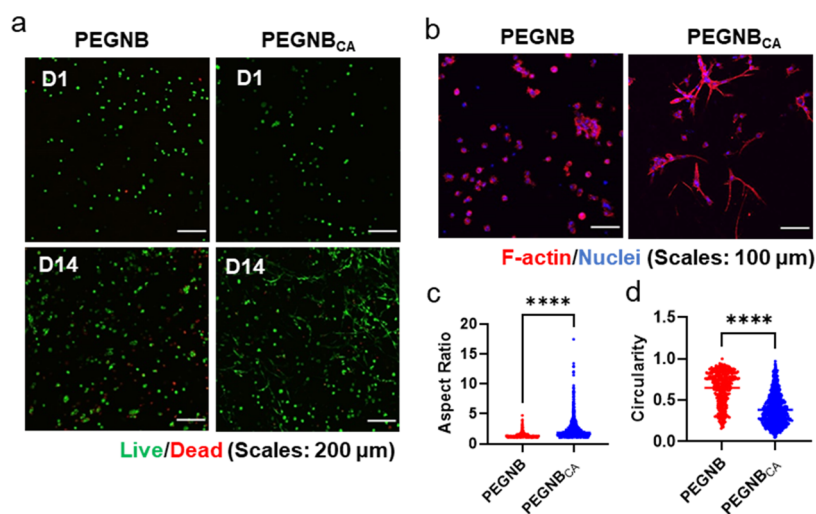


Figure 5. Cytocompatibility of PEGNB_{CA} iEDDA click cross-linked hydrogels. (a) Representative confocal images of live/dead stained hMSCs encapsulated in 2.5 wt % PEGNB_{CA}-based iEDDA hydrogels cross-linked with PEG-35mTz/65Tz at R = 0.5 with 3 wt % Gel-50mTz/50Tz. (b) Representative F-actin staining confocal images (day 14). hMSCs were encapsulated in 2.5 wt % PEGNB_{CA}. (c) Aspect ratio. (d) Circularity (c, d results obtained from F-actin staining images).

the two sets of hydrogels contained the same amount of gelatin, we reasoned that the spreading morphology observed in PEGNB_{CA} hydrogels relative to PEGNB hydrogels may be attributed to accelerated hydrolysis.

In Vivo Performance of iEDDA Click Cross-linked PEG Hydrogels. To demonstrate the injectability, 2.5 wt % PEGNB_{CA} R = 0.8 cross-linked with PEG-35mTz/65Tz was

preincubated at 37 °C for 10 min followed by injection into a star mold using a 23 G needle. Less than 10 min later, a gel was formed (Figure S8). To test the in vivo biocompatibility of the iEDDA click cross-linked PEGNB_{CA} hydrogels, 2.5 wt % PEGNB_{CA} or PEGNB cross-linked with PEG-35mTz/65Tz was injected subcutaneously into the left hindlimb of C57BL/6 mice. After two weeks, the mice were sacrificed and

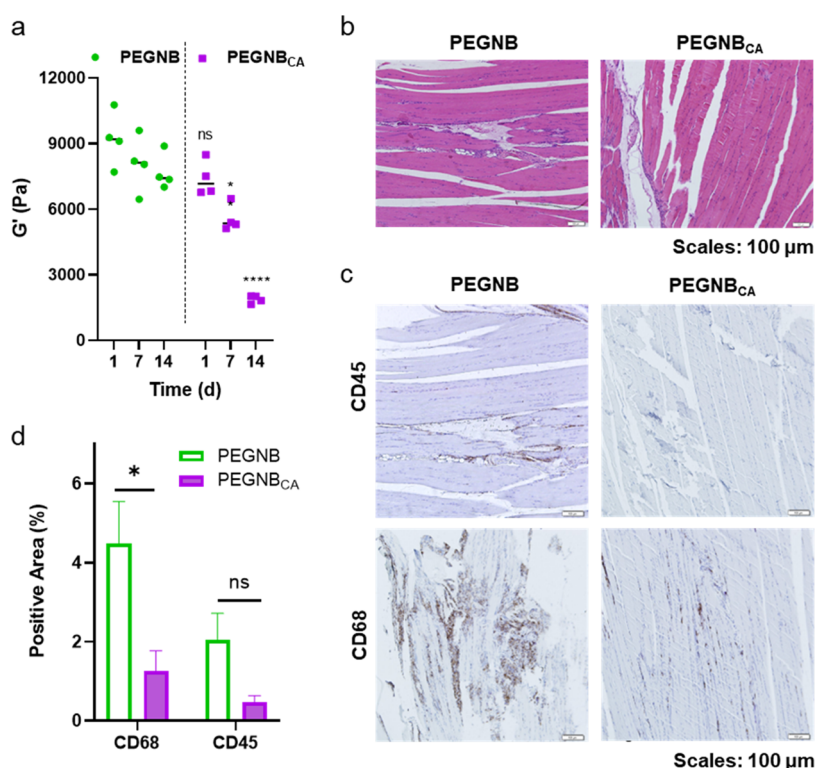


Figure 6. Biocompatibility of PEGNB_{CA} iEDDA click cross-linked hydrogels. (a) Shear moduli of 2.5 wt % PEGNB or PEGNB_{CA} hydrogels ($R = 0.8$) cross-linked with PEG-35mTz/65Tz, with 3 wt % Gel-50mTz/50Tz. (b, c) In vivo tissue response to injectable PEG-based iEDDA hydrogels. At 14 days post injection, tissues were explanted and subjected to immunohistochemical staining using (b) hematoxylin and eosin (H&E) and (c) anti-CD68 and anti-CD45 antibodies. (d) Semiquantitative analysis of histology sections stained positive with CD68 and CD45.

immunohistochemical staining (H&E, CD45, and CD68) was performed. No remnants of PEGNB_{CA} hydrogels were present in any of the histology samples, indicating complete degradation of the hydrogel before sample recovery. Gel fragments of PEGNB hydrogels were present in two of the three samples (Figure S9). While the initial elastic moduli of the injected iEDDA PEGNB or PEGNB_{CA} hydrogels were similar (Figure 6a), after 14 days the average elastic moduli of PEGNB_{CA} hydrogels decreased to ~ 2 kPa, while those of PEGNB hydrogels were significantly higher (~ 7.5 kPa, Figure 6a). No noticeable difference in H&E staining of the tissue was observed between the two conditions, as shown in the microscope images (Figure 6b). CD68 and CD45 staining of histology samples showed higher macrophage and lymphocyte activity, respectively, in the PEGNB condition compared to PEGNB_{CA} (Figure 6c). Image analysis showed a higher percent positive area of CD68 and CD45 images of the histology samples with PEGNB hydrogel compared to PEGNB_{CA} (Figure 6d). In fact, the CD68 percent positive area was statistically higher in the histology samples with the PEGNB hydrogel compared to the PEGNB_{CA} hydrogel.

DISCUSSION

PEG-based hydrogels with engineered functionality (e.g., inclusion of cell adhesive motifs and protease-labile linkages) and degradability (e.g., hydrolysis, proteolysis, photolysis, etc.) are invaluable in tissue engineering and drug delivery applications.^{23–25} For example, hydrolytically degradable PEG hydrogels have been used for sustained-release applications of therapeutics and proteins for wound healing^{26–28} and cartilage repair.²⁹ In particular, norbornene-

functionalized PEG (i.e., PEGNB) is increasingly used in PEG-based hydrogel fabrication owing to its high cytocompatibility and dual reactivity towards thiol (in thiol-NB click reactions) and (m)Tz (NB-(m)Tz click reactions).^{4,7,30} We have previously reported an alternative PEGNB synthesis protocol using CA,¹⁹ an odorless diacid anhydride containing the NB derivative. CA was conjugated onto PEG terminal hydroxyl groups via esterification using DMAP as a catalyst. The CA underwent cyclic desymmetrization, yielding PEGNB_{CA}, a functional macromer with the norbornene group and a carboxylic acid that can be utilized for additional functionalization (Figure 1a).³¹ Successful synthesis of PEGNB_{CA} and PEGTz/PEG-mTz permitted bio-orthogonal hydrogel cross-linking via the iEDDA click reaction (Figure 1c). Our previous work showed that thiol-norbornene photoclick hydrogels cross-linked by PEGNB degraded slowly owing to the slow ester hydrolysis kinetics.⁶ We also showed that replacing the ester linkage with an amide bond (i.e., PEGNB synthesized by PEG-amine) led to thiol-norbornene hydrogels resistant to hydrolysis under ambient conditions.³² Later, we showed that upon cross-linking into hydrogels, PEGNB_{CA}-based hydrogels displayed unexpected fast hydrolytic degradation kinetics,¹⁹ presumably a result of the accelerated hydrolysis of the ester linkages caused by the neighboring carboxylic acid. We expected a similar accelerated hydrolytic hydrogel degradation when PEGNB_{CA} was used to cross-link PEGTz or PEG-mTz via the iEDDA click reaction (Figure 2a).

While both PEGNB and PEGNB_{CA} provided norbornene moiety for iEDDA click hydrogel cross-linking, the presence of carboxylic acid on PEGNB_{CA} appeared to slightly reduce the iEDDA hydrogel cross-linking efficiency (Figure 1e). In

addition to PEGNB and PEGNB_{CA}, we synthesized two Tz cross-linkers, PEGTz and PEG-mTz, and examined the hydrolytic stability of these four sets of iEDDA click hydrogels over 80 days (Figure 2b). We found that PEGNB + PEGTz hydrogels exhibited exceptional hydrolytic stability with no noticeable degradation over 80 days. The result, consistent with the literature, was attributed to the relative stability of PEGNB-ester bonds formed by Steglich esterification, as well as the secondary noncovalent bonding between the NB-Tz adducts.^{33,34} Interestingly, iEDDA click hydrogels cross-linked by PEG-mTz (PEGNB + PEG-mTz group) underwent gradual stiffening (20% higher G') and subsequently showed significant hydrolytic degradation in the first 45 days, followed by a less pronounced degradation afterward. The initial 20% increase in G' when PEG-mTz was used could be attributed to the slower reaction kinetics between NB and mTz motifs (Figure 1d). Following gelation, we reasoned that the presence of the additional methyl group on mTz disrupted the supramolecular interactions otherwise observed in the PEGNB + PEGTz hydrogels, hence permitting the hydrolytic degradation of ester bonds on PEGNB to dominate the structural instability of the PEGNB + PEG-mTz hydrogels. Of note, the supramolecular interactions formed between Tz-NB adducts following the iEDDA click reaction has been reported through experimental efforts and molecular dynamic simulations.⁷ Our results not only corroborate the literature, but also provide additional insights into the cross-linking and degradation of iEDDA click hydrogels using mTz-conjugated macromers.

We next examined the hydrolytic degradation of PEGNB_{CA}-based iEDDA click hydrogels and found that replacing PEGNB with PEGNB_{CA} resulted in significant acceleration of hydrogel degradation, regardless of the PEGTz or PEG-mTz cross-linker. It is likely that the additional neighboring carboxylic acid on PEGNB_{CA} prevented or reduced the supramolecular interactions otherwise formed between NB and Tz adducts. Additionally, the presence of the neighboring carboxylic acid was believed to accelerate the hydrolysis rate of the ester bond as we have reported previously.¹⁹ The degradation was not pH-dependent as no noticeable difference in hydrogel degradation was observed when buffered solutions of pH 2 to pH 12 were used (data not shown). Through exponential pseudo-first-order decay fitting of the shear moduli data over time,^{6,19} we showed that the k_{hyd} for PEGNB_{CA} + PEGTz was more than twice faster than that for the PEGNB_{CA} + PEG-mTz group (Table 1). While the additional methyl groups on mTz promoted degradation of PEGNB-based iEDDA click hydrogels (due to disruption of π - π stacking),^{33,34} they reduced the degradation rate of PEGNB_{CA}-based hydrogels. In the absence of supramolecular interactions otherwise formed between NB and Tz (due to the neighboring carboxylic acid group on PEGNB_{CA}), the presence of hydrophobic mTz appeared to reduce the ester bond hydrolysis.³⁵ Taken together, we have presented the first group of PEG-based iEDDA click hydrogels with pre-engineered hydrolytic degradability.

To further explore the tunability of hydrolytically degradable iEDDA click hydrogels, we synthesized dually modified mTz/Tz PEG to control the gelation and degradation kinetics. It is known that through the addition of electron-withdrawing groups on the dienophile (i.e., norbornene) and electron-donating groups on the diene (i.e., tetrazine), the reaction kinetics are slowed.³⁶ Thus, we expected PEGNB_{CA} iEDDA click cross-linked hydrogels to have slower gelation times

compared to the equivalent PEGNB hydrogels (Figure 3b). Further, previous studies have shown that hydrogels cross-linked with mTz have slower gelation times compared to the same hydrogels cross-linked with Tz.⁵ Due to this, we decided to functionalize Tz and mTz on the same polymer to allow for decreased gelation time by the fast-reacting tetrazine to form the hydrogel initially, so that the mTz/NB reaction can occur within the hydrogel network over time. This design would leave sufficient time for material preparation in injectable delivery applications while reducing cell sedimentation during the encapsulation.³⁷ For all of the three cross-linkers, relatively quick gelation times were achieved (in under 20 min; Figure 3c), which is faster than that of traditional Diels–Alder reactions.³⁷ As shown previously,^{5,38} the gelation time of iEDDA click cross-linked PEGNB_{CA} hydrogels is temperature sensitive, with a quicker gelation time at physiological temperature compared to room temperature (Figure 3d), making them ideal for injectable applications. Compared to thiol-norbornene cross-linking,¹⁹ a much lower PEG macromer concentration is needed to achieve high elastic moduli, which is consistent with the literature (Figure 3e,f).⁷ Further, at low macromer concentrations with R ratio equal to 1, increased shear moduli of iEDDA click cross-linked hydrogels were observed after day 0, indicating that the increase in stiffness is possibly from the slow reaction kinetics of mTz or from the delayed supramolecular interactions from the tetrazine adducts.^{7,8} Due to this, we envisioned that this hydrogel system may be useful in studying the effect of dynamic stiffening and subsequent softening on cell fate without external stimuli such as light or enzyme.^{39–41} A highly tunable degradation was achieved through the PEG-mTz/Tz ratio cross-linkers, with the higher ratio of mTz degrading slower across all different formulations (Figure 4c–h). A higher degree of stiffening was observed when the gels were fabricated with a lower polymer concentration as these gels were softer and more amenable to supramolecular interactions. However, these gels still exhibited hydrolytic degradation once they reached the maximum degree of stiffening. Further, all conditions adhered closely to the pseudo-first-order kinetics by having R^2 values greater than 0.93, excluding 1.75 wt % PEGNB_{CA} cross-linked with PEG-35mTz/65Tz at $R = 1$, and displayed a wide range of degradation from 11 days to over 90 days (Table S1). Future work will focus on developing a mathematical model to predict the hydrolytic degradation of PEG-based iEDDA click hydrogels.^{42,43}

Due to their prevalence in tissue engineering and mechanobiology,^{44–47} hMSCs were chosen to assess the cytocompatibility and morphology within the slow-degrading PEGNB and fast-degrading PEGNB_{CA} iEDDA click cross-linked hydrogels. Within a degrading matrix, we have shown that hMSCs display a spreading morphology, while in a statically stiff matrix, hMSCs maintain a round morphology.⁴⁸ Similarly, we saw that hMSCs within the hydrolytically degradable PEGNB_{CA}-based iEDDA click hydrogels exhibited a spreading morphology, whereas hMSCs within the non-degradable hydrogels maintained a spherical morphology. Of note, in both hydrogels, mTz/Tz functionalized (50:50) gelatin was added to promote cell adhesion and protease-labile sites. Due to the ease of functionalizing (m)Tz onto biopolymers (i.e., gelatin and hyaluronic acid),^{13–15,38} we envision this system to be highly adaptable for creating modular and biomimetic matrices. Future studies may utilize this hydrogel system to observe the effect of dynamic stiffening

using Tz/NB chemistry with subsequent softening from hydrolysis on stem cell differentiation and changes in suture.^{49,50}

The spontaneous reaction of Tz/NB iEDDA click chemistry is ideal for biomedical applications owing to its specific and high reactivity under ambient conditions without the need of external stimuli. In particular, this chemistry has been applied for in vivo applications including fluorescent imaging,^{51,52} ligation of biomolecules,^{53,54} and injectable, covalently cross-linked hydrogels.^{17,55–57} Due to the fast gelation time and predictable degradation, we envision PEGNB_{CA} iEDDA click cross-linked hydrogels to be ideal for injectable hydrogel for delivery applications. Due to the degrading matrix, we anticipated a lesser degree of immune response compared to the statically stiff PEGNB hydrogels, consistent with the literature.⁵⁸ Overall, PEGNB_{CA} iEDDA click cross-linked hydrogels produced less of an inflammatory response, as indicated by the CD45 and CD68 staining and subsequent image analysis (Figure 6c,d). Future studies of the PEGNB_{CA} iEDDA click cross-linked hydrogels can include further functionalization to improve the injectability by adding either a second network that displays shear-thinning compatibilities or a thermosensitive functional group.^{59–62} Further, since the injectable hydrogel system displayed excellent cytocompatibility with hMSCs and can be further functionalized through norbornene chemistry, applications in injectable cell delivery of hMSCs for musculoskeletal regeneration should be explored.

CONCLUSIONS

We have developed the first hydrolytically degradable PEG-based iEDDA click hydrogels with pre-engineered and highly tunable degradation kinetics. Accelerated hydrogel degradation was conferred by the new PEGNB_{CA} macromer cross-linked with the PEG-(m)Tz via iEDDA reaction. PEGNB_{CA} + PEG-mTz hydrogels displayed a two times slower rate of hydrolysis compared to PEGNB_{CA} + PEGTz. Due to this difference, mTz/Tz cross-linkers were synthesized and cross-linked with PEGNB_{CA}, proving that the ratio of mTz/Tz is an effective method for achieving a wide range of degradation from a few weeks to more than several months. The iEDDA click cross-linked PEGNB_{CA} hydrogels were highly cytocompatible in vitro and displayed a spreading morphology of hMSCs most likely due to the accelerated hydrolysis. Further, the new iEDDA hydrogels were capable of being injected and were highly compatible in vivo. We expect that this new PEG-based iEDDA hydrogel system will contribute to the field of degradable hydrogels for tissue regeneration and drug/cell delivery applications.

ASSOCIATED CONTENT

Supporting Information

The Supporting Information is available free of charge at <https://pubs.acs.org/doi/10.1021/acsbomaterials.2c00714>.

Additional information about how gel fraction, swelling ratio, and mesh size was calculated; additional figures include NMR spectrums of PEGNB, PEGNB_{CA}, and PEG-mTz/Tz; graphs of gel fraction, swelling ratio over time, and mesh size calculations of PEG-based iEDDA click hydrogels; histology analysis and additional images of injected iEDDA cross-linked PEG/Gelatin hybrid hydrogels; additionally, table containing results from

exponential decay fitting of the PEGNB_{CA} cross-linked with dual-functional PEG-mTz/Tz (PDF)

AUTHOR INFORMATION

Corresponding Author

Chien-Chi Lin – Department of Biomedical Engineering, Purdue School of Engineering & Technology, Indiana University-Purdue University Indianapolis, Indianapolis, Indiana 46202, United States; orcid.org/0000-0002-4175-8796; Phone: (317) 274-0760; Email: lincc@iupui.edu

Authors

Nathan H. Dimmitt – Department of Biomedical Engineering, Purdue School of Engineering & Technology, Indiana University-Purdue University Indianapolis, Indianapolis, Indiana 46202, United States

Matthew R. Arkenberg – Weldon School of Biomedical Engineering, Purdue University, West Lafayette, Indiana 47907, United States

Mariana Moraes de Lima Perini – Department of Biology, Purdue School of Science, Indiana University-Purdue University Indianapolis, Indianapolis, Indiana 46202, United States

Jiliang Li – Department of Biology, Purdue School of Science, Indiana University-Purdue University Indianapolis, Indianapolis, Indiana 46202, United States

Complete contact information is available at:

<https://pubs.acs.org/10.1021/acsbomaterials.2c00714>

Notes

The authors declare no competing financial interest.

ACKNOWLEDGMENTS

This work was supported in part by the National Institutes of Health (R01CA227737 and R01DK127436 to CCL) and (R01AG060621 to JL). The authors thank Mr. Drew Brown and the Histology Core at Indiana University School of Medicine for assistance in the immunohistochemistry staining service.

REFERENCES

- (1) Tang, S.; Richardson, B. M.; Anseth, K. S. Dynamic covalent hydrogels as biomaterials to mimic the viscoelasticity of soft tissues. *Prog. Mater. Sci.* **2021**, *120*, No. 100738.
- (2) Hansell, C. F.; Espeel, P.; Stamenovic, M. M.; Barker, I. A.; Dove, A. P.; Du Prez, F. E.; O'Reilly, R. K. Additive-free clicking for polymer functionalization and coupling by tetrazine–norbornene chemistry. *J. Am. Chem. Soc.* **2011**, *133*, 13828–13831.
- (3) Blackman, M. L.; Royzen, M.; Fox, J. M. Tetrazine ligation: fast bioconjugation based on inverse-electron-demand Diels–Alder reactivity. *J. Am. Chem. Soc.* **2008**, *130*, 13518–13519.
- (4) Arkenberg, M. R.; Dimmitt, N. H.; Johnson, H. C.; Koehler, K. R.; Lin, C. C. Dynamic Click Hydrogels for Xeno-Free Culture of Induced Pluripotent Stem Cells. *Adv. Biosyst.* **2020**, *4*, No. 2000129.
- (5) Ziegler, C. E.; Graf, M.; Nagaoka, M.; Lehr, H.; Goeperich, A. M. In Situ Forming iEDDA Hydrogels with Tunable Gelation Time Release High-Molecular Weight Proteins in a Controlled Manner over an Extended Time. *Biomacromolecules* **2021**, *22*, 3223–3236.
- (6) Shih, H.; Lin, C.-C. Cross-linking and degradation of step-growth hydrogels formed by thiol–ene photoclick chemistry. *Biomacromolecules* **2012**, *13*, 2003–2012.
- (7) Holt, S. E.; Rakoski, A.; Jivan, F.; Pérez, L. M.; Alge, D. L. Hydrogel Synthesis and Stabilization via Tetrazine Click-Induced

Secondary Interactions. *Macromol. Rapid Commun.* **2020**, *41*, No. 2000287.

(8) Holt, S. E.; Arroyo, J.; Poux, E.; Fricks, A.; Agurcia, I.; Heintschel, M.; Rakoski, A.; Alge, D. L. Supramolecular Click Product Interactions Induce Dynamic Stiffening of Extracellular Matrix-Mimetic Hydrogels. *Biomacromolecules* **2021**, *22*, 3040–3048.

(9) Alge, D. L.; Azagarsamy, M. A.; Donohue, D. F.; Anseth, K. S. Synthetically tractable click hydrogels for three-dimensional cell culture formed using tetrazine–norbornene chemistry. *Biomacromolecules* **2013**, *14*, 949–953.

(10) Desai, R. M.; Koshy, S. T.; Hilderbrand, S. A.; Mooney, D. J.; Joshi, N. S. Versatile click alginate hydrogels crosslinked via tetrazine–norbornene chemistry. *Biomaterials* **2015**, *50*, 30–37.

(11) Lueckgen, A.; Garske, D. S.; Ellinghaus, A.; Mooney, D. J.; Duda, G. N.; Cipitria, A. Enzymatically-degradable alginate hydrogels promote cell spreading and in vivo tissue infiltration. *Biomaterials* **2019**, *217*, No. 119294.

(12) Lueckgen, A.; Garske, D. S.; Ellinghaus, A.; Mooney, D. J.; Duda, G. N.; Cipitria, A. Dual alginate crosslinking for local patterning of biophysical and biochemical properties. *Acta Biomater.* **2020**, *115*, 185–196.

(13) Contessi Negrini, N.; Angelova Volponi, A.; Sharpe, P. T.; Celiz, A. D. Tunable Cross-Linking and Adhesion of Gelatin Hydrogels via Bioorthogonal Click Chemistry. *ACS Biomater. Sci. Eng.* **2021**, *7*, 4330–4346.

(14) Koshy, S. T.; Desai, R. M.; Joly, P.; Li, J.; Bagrodia, R. K.; Lewin, S. A.; Joshi, N. S.; Mooney, D. J. Click-crosslinked injectable gelatin hydrogels. *Adv. Healthcare Mater.* **2016**, *5*, 541–547.

(15) Delplace, V.; Nickerson, P. E.; Ortin-Martinez, A.; Baker, A. E.; Wallace, V. A.; Shoichet, M. S. Nonswelling, Ultralow Content Inverse Electron-Demand Diels–Alder Hyaluronan Hydrogels with Tunable Gelation Time: Synthesis and In Vitro Evaluation. *Adv. Funct. Mater.* **2020**, *30*, No. 1903978.

(16) Delplace, V.; Pickering, A. J.; Hettiaratchi, M. H.; Zhao, S.; Kivijärvi, T.; Shoichet, M. S. Inverse electron-demand diels–alder methylcellulose hydrogels enable the Co-delivery of chondroitinase ABC and neural progenitor cells. *Biomacromolecules* **2020**, *21*, 2421–2431.

(17) Vu, T. T.; Gulfam, M.; Jo, S.-H.; Park, S.-H.; Lim, K. T. Injectable and biocompatible alginate-derived porous hydrogels cross-linked by IEDDA click chemistry for reduction-responsive drug release application. *Carbohydr. Polym.* **2022**, *278*, No. 118964.

(18) Lueckgen, A.; Garske, D. S.; Ellinghaus, A.; Desai, R. M.; Stafford, A. G.; Mooney, D. J.; Duda, G. N.; Cipitria, A. Hydrolytically-degradable click-crosslinked alginate hydrogels. *Biomaterials* **2018**, *181*, 189–198.

(19) Lin, F.-Y.; Lin, C.-C. Facile synthesis of rapidly degrading peg-based thiol-norbornene hydrogels. *ACS Macro Lett.* **2021**, *10*, 341–345.

(20) Fairbanks, B. D.; Schwartz, M. P.; Halevi, A. E.; Nuttelman, C. R.; Bowman, C. N.; Anseth, K. S. A versatile synthetic extracellular matrix mimic via thiol-norbornene photopolymerization. *Adv. Mater.* **2009**, *21*, 5005–5010.

(21) Lin, C.-C.; Raza, A.; Shih, H. PEG hydrogels formed by thiolene photo-click chemistry and their effect on the formation and recovery of insulin-secreting cell spheroids. *Biomaterials* **2011**, *32*, 9685–9695.

(22) Jiang, Z.; Lin, F.-Y.; Jiang, K.; Nguyen, H.; Chang, C.-Y.; Lin, C.-C. Dissolvable microgel-templated macroporous hydrogels for controlled cell assembly. *Biomater. Adv.* **2022**, No. 112712.

(23) Zou, Y.; Zhang, L.; Yang, L.; Zhu, F.; Ding, M.; Lin, F.; Wang, Z.; Li, Y. “Click” chemistry in polymeric scaffolds: Bioactive materials for tissue engineering. *J. Controlled Release* **2018**, *273*, 160–179.

(24) Arkenberg, M. R.; Nguyen, H. D.; Lin, C.-C. Recent advances in bio-orthogonal and dynamic crosslinking of biomimetic hydrogels. *J. Mater. Chem. B* **2020**, *8*, 7835–7855.

(25) Lin, C.-C.; Korc, M. Designer hydrogels: Shedding light on the physical chemistry of the pancreatic cancer microenvironment. *Cancer Lett.* **2018**, *436*, 22–27.

(26) Jain, E.; Sheth, S.; Dunn, A.; Zustiak, S. P.; Sell, S. A. Sustained release of multicomponent platelet-rich plasma proteins from hydrolytically degradable PEG hydrogels. *J. Biomed. Mater. Res., Part A* **2017**, *105*, 3304–3314.

(27) Zustiak, S. P.; Leach, J. B. Characterization of protein release from hydrolytically degradable poly (ethylene glycol) hydrogels. *Biotechnol. Bioeng.* **2011**, *108*, 197–206.

(28) Kwak, G.; Cheng, J.; Kim, H.; Song, S.; Lee, S. J.; Yang, Y.; Jeong, J. H.; Lee, J. E.; Messersmith, P. B.; Kim, S. H. Sustained Exosome-Guided Macrophage Polarization Using Hydrolytically Degradable PEG Hydrogels for Cutaneous Wound Healing: Identification of Key Proteins and MiRNAs, and Sustained Release Formulation. *Small* **2022**, *18*, No. 2200060.

(29) Skaalure, S. C.; Dimson, S. O.; Pennington, A. M.; Bryant, S. J. Semi-interpenetrating networks of hyaluronic acid in degradable PEG hydrogels for cartilage tissue engineering. *Acta Biomater.* **2014**, *10*, 3409–3420.

(30) Jivan, F.; Yegappan, R.; Pearce, H.; Carrow, J. K.; McShane, M.; Gaharwar, A. K.; Alge, D. L. Sequential thiol–ene and tetrazine click reactions for the polymerization and functionalization of hydrogel microparticles. *Biomacromolecules* **2016**, *17*, 3516–3523.

(31) Muthusamy, S.; Gnanaprakasam, B.; Suresh, E. Desymmetrization of cyclic anhydrides using dihydroxy compounds: Selective synthesis of macrocyclic tetralactones. *Org. Lett.* **2006**, *8*, 1913–1916.

(32) Raza, A.; Lin, C. C. The Influence of Matrix Degradation and Functionality on Cell Survival and Morphogenesis in PEG-Based Hydrogels. *Macromol. Biosci.* **2013**, *13*, 1048–1058.

(33) Moses Abraham, B.; Prathap Kumar, J.; Vaitheeswaran, G. High-pressure studies of hydrogen-bonded energetic material 3, 6-dihydrazino-s-tetrazine using DFT. *ACS omega* **2018**, *3*, 9388–9399.

(34) Odelius, M.; Kirchner, B.; Hutter, J. s-Tetrazine in aqueous solution: A density functional study of hydrogen bonding and electronic excitations. *J. Phys. Chem. A* **2004**, *108*, 2044–2052.

(35) Kroger, S. M.; Hill, L.; Jain, E.; Stock, A.; Bracher, P. J.; He, F.; Zustiak, S. P. Design of hydrolytically degradable polyethylene glycol crosslinkers for facile control of hydrogel degradation. *Macromol. Biosci.* **2020**, *20*, No. 2000085.

(36) Oliveira, B. L.; Guo, Z.; Bernardes, G. Inverse electron demand Diels–Alder reactions in chemical biology. *Chem. Soc. Rev.* **2017**, *46*, 4895–4950.

(37) Madl, C. M.; Heilshorn, S. C. Rapid Diels–Alder cross-linking of cell encapsulating hydrogels. *Chem. Mater.* **2019**, *31*, 8035–8043.

(38) Famili, A.; Rajagopal, K. Bio-orthogonal cross-linking chemistry enables in situ protein encapsulation and provides sustained release from hyaluronic acid based hydrogels. *Mol. Pharmaceutics* **2017**, *14*, 1961–1968.

(39) Zheng, Z.; Hu, J.; Wang, H.; Huang, J.; Yu, Y.; Zhang, Q.; Cheng, Y. Dynamic softening or stiffening a supramolecular hydrogel by ultraviolet or near-infrared light. *ACS Appl. Mater. Interfaces* **2017**, *9*, 24511–24517.

(40) Perera, M. M.; Chimala, P.; Elhusain-Elnegres, A.; Heaton, P.; Ayres, N. Reversibly Softening and Stiffening Organogels Using a Wavelength-Controlled Disulfide-Diselenide Exchange. *ACS Macro Lett.* **2020**, *9*, 1552–1557.

(41) Arkenberg, M. R.; Moore, D. M.; Lin, C.-C. Dynamic control of hydrogel crosslinking via sortase-mediated reversible transpeptidation. *Acta Biomater.* **2019**, *83*, 83–95.

(42) Weber, L. M.; Lopez, C. G.; Anseth, K. S. Effects of PEG hydrogel crosslinking density on protein diffusion and encapsulated islet survival and function. *J. Biomed. Mater. Res., Part A* **2009**, *90A*, 720–729.

(43) Axpe, E.; Chan, D.; Offeddu, G. S.; Chang, Y.; Merida, D.; Hernandez, H. L.; Appel, E. A. A multiscale model for solute diffusion in hydrogels. *Macromolecules* **2019**, *52*, 6889–6897.

(44) Choi, J. R.; Yong, K. W.; Choi, J. Y. Effects of mechanical loading on human mesenchymal stem cells for cartilage tissue engineering. *J. Cell. Physiol.* **2018**, *233*, 1913–1928.

- (45) Vasanthan, J.; Gurusamy, N.; Rajasingh, S.; Sigamani, V.; Kirankumar, S.; Thomas, E. L.; Rajasingh, J. Role of human mesenchymal stem cells in regenerative therapy. *Cells* **2021**, *10*, 54.
- (46) Hao, J.; Zhang, Y.; Jing, D.; Shen, Y.; Tang, G.; Huang, S.; Zhao, Z. Mechanobiology of mesenchymal stem cells: perspective into mechanical induction of MSC fate. *Acta Biomater.* **2015**, *20*, 1–9.
- (47) Zhang, Y.; Chen, H.; Zhang, T.; Zan, Y.; Ni, T.; Liu, M.; Pei, R. Fast-forming BMSC-encapsulating hydrogels through bioorthogonal reaction for osteogenic differentiation. *Biomater. Sci.* **2018**, *6*, 2578–2581.
- (48) Hao, Y.; Shih, H.; Muñoz, Z.; Kemp, A.; Lin, C.-C. Visible light cured thiol-vinyl hydrogels with tunable degradation for 3D cell culture. *Acta Biomater.* **2014**, *10*, 104–114.
- (49) Guvendiren, M.; Burdick, J. A. Stiffening hydrogels to probe short-and long-term cellular responses to dynamic mechanics. *Nat. Commun.* **2012**, *3*, No. 792.
- (50) Wechsler, M. E.; Rao, V. V.; Borelli, A. N.; Anseth, K. S. Engineering the MSC secretome: a hydrogel focused approach. *Adv. Healthcare Mater.* **2021**, *10*, No. 2001948.
- (51) Knight, J. C.; Richter, S.; Wuest, M.; Way, J. D.; Wuest, F. Synthesis and evaluation of an 18 F-labelled norbornene derivative for copper-free click chemistry reactions. *Org. Biomol. Chem.* **2013**, *11*, 3817–3825.
- (52) Devaraj, N. K.; Weissleder, R. Biomedical applications of tetrazine cycloadditions. *Acc. Chem. Res.* **2011**, *44*, 816–827.
- (53) Knall, A.-C.; Slugovc, C. Inverse electron demand Diels–Alder (iEDDA)-initiated conjugation: a (high) potential click chemistry scheme. *Chem. Soc. Rev.* **2013**, *42*, 5131–5142.
- (54) Peuler, K.; Dimmitt, N.; Lin, C.-C. Clickable modular polysaccharide nanoparticles for selective cell-targeting. *Carbohydr. Polym.* **2020**, *234*, No. 115901.
- (55) Zhang, Z.; He, C.; Chen, X. Injectable click polypeptide hydrogels via tetrazine-norbornene chemistry for localized cisplatin release. *Polymers* **2020**, *12*, 884.
- (56) Gulfam, M.; Jo, S.-H.; Jo, S.-W.; Vu, T. T.; Park, S.-H.; Lim, K. T. Highly porous and injectable hydrogels derived from cartilage acellularized matrix exhibit reduction and NIR light dual-responsive drug release properties for application in antitumor therapy. *NPG Asia Mater.* **2022**, *14*, No. 8.
- (57) Hoang, H. T.; Jo, S.-H.; Phan, Q.-T.; Park, H.; Park, S.-H.; Oh, C.-W.; Lim, K. T. Dual pH-/thermo-responsive chitosan-based hydrogels prepared using “click” chemistry for colon-targeted drug delivery applications. *Carbohydr. Polym.* **2021**, *260*, No. 117812.
- (58) Bédouet, L.; Pascale, F.; Moine, L.; Wassef, M.; Ghegediban, S. H.; Nguyen, V.-N.; Bonneau, M.; Labarre, D.; Laurent, A. Intra-articular fate of degradable poly (ethyleneglycol)-hydrogel microspheres as carriers for sustained drug delivery. *Int. J. Pharm.* **2013**, *456*, 536–544.
- (59) Guvendiren, M.; Lu, H. D.; Burdick, J. A. Shear-thinning hydrogels for biomedical applications. *Soft Matter* **2012**, *8*, 260–272.
- (60) Lin, F.-Y.; Dimmitt, N. H.; Moraes de Lima Perini, M.; Li, J.; Lin, C.-C. Injectable Acylhydrazone-Linked RAFT Polymer Hydrogels for Sustained Protein Release and Cell Encapsulation. *Adv. Healthcare Mater.* **2022**, No. 2101284.
- (61) Alexander, A.; Ajazuddin; Khan, J.; Saraf, S.; Saraf, S. Polyethylene glycol (PEG)–Poly (N-isopropylacrylamide)- (PNIPAAm) based thermosensitive injectable hydrogels for biomedical applications. *Eur. J. Pharm. Biopharm.* **2014**, *88*, 575–585.
- (62) Alexander, A.; Ajazuddin; Khan, J.; Saraf, S.; Saraf, S. Poly (ethylene glycol)–poly (lactic-co-glycolic acid) based thermosensitive injectable hydrogels for biomedical applications. *J. Controlled Release* **2013**, *172*, 715–729.